

Received:

6 June 2017

Revised:

6 September 2017

Accepted:

28 December 2017

Cite as: J. Sackey, K.A. Dompseh, B. Mothudi, M. Maaza. Theoretical study of electromagnetic transport in Lepidoptera *Danaus plexippus* wing scales. Heliyon 4 (2018) e00502. doi: 10.1016/j.heliyon.2017.e00502



# Theoretical study of electromagnetic transport in Lepidoptera *Danaus plexippus* wing scales

J. Sackey<sup>b,c,\*</sup>, K.A. Dompseh<sup>a,b</sup>, B. Mothudi<sup>c</sup>, M. Maaza<sup>b,c</sup>

<sup>a</sup> Department of Physics, University of Cape Coast, Ghana

<sup>b</sup> Nanosciences African Network (NANOAFNET), iThemba LABS Somerset West, Western Cape Province, South Africa

<sup>c</sup> University of South Africa (UNISA), Muckleneuk Ridge, P.O. Box 392, Pretoria, South Africa

\* Corresponding author.

E-mail address: sackey@tlabs.ac.za (J. Sackey).

## Abstract

This paper examines the electromagnetic energies developed in the scales of the Lepidoptera *Danaus plexippus*. The Green tensor method was used to calculate and simulate the energies at specific wavelengths. Scattering of electromagnetic waves within the scales was simulated at different wavelengths ( $\lambda$ ) with the corresponding maximum energy occurred at  $\lambda = 0.45 \mu\text{m}$ . The study shows that the design of wing's cross-ribs maximizes the eigenmode of electromagnetic energy. This shows promising applications in bio-sensors of Solar light and likewise in waveguide for photonic transmission.

Keywords: Materials science, Engineering, Nanotechnology

## 1. Introduction

Butterfly wings are natural photonic nanostructures with characteristics of being multifunctional and energy-chemical elements. The wings exhibit complex architecture having hierarchical structures with voids ranging from 100 nm to a few micrometers [1, 2, 3]. Colours on the butterfly wings originate either from pigmentation or structural mechanism. The structural mechanism found on most butterflies is adopted in bio-mimics of waveguides for photonic transmission. Most

authors use the Fourier Model Methods (FMM) [4, 5] to study the interaction of light with the wings by discretizing the wing structure along the wave propagation direction. Next, is to impose a boundary condition to get the eigenmodes of electromagnetic waves. The drawback to this method is that it leads to exponentially growing evanescence modes. Yet to compute fields in and around the scales, the Green tensor method is applicable. The Green tensor method is a solution for a point source of the wave equation and it enables the computation of fields in and around the scales (known as the scatter) using a matrix method.

In this study, we applied Green tensor method to calculate the energy of light traveling within the grooves (wings scales) of *Danaus plexippus* butterfly. The *Danaus plexippus* butterflies are of order Lepidoptera belonging to Nymphalidae families. This butterfly combines flapping and gliding of its wings to move from place to place [6]; Navigation is an important aspect of this Lepidoptera species. The flight abilities of this butterfly are of much importance due to the range of distances they can travel which has earned them the name “the wanderer” [7, 8]. Studies conducted on the Lepidoptera suggest that they use the eyes as photo-receptors in detecting polarized light in the ultraviolet region [9]. Interaction of polarized light in the region close to an ultraviolet spectrum with the wing is important [10]. In this study, we use Green tensor function to reveal the interaction of light with the wing. The arrangement of paper is: (i) scattering of polarized light in and around the wing using the Green tensor method [11, 12], (ii) computational analysis of scattered wave in the grooves and corresponding electromagnetic energies.

## 2. Background

In Fig. 1(a), the wing of the *Danaus plexippus* butterfly displays beautiful colour combination of reddish-orange with black vein-like markings and white spots. The scatter plot of segmented pixels in  $a^*b^*$  space shows a mapping of colors in the

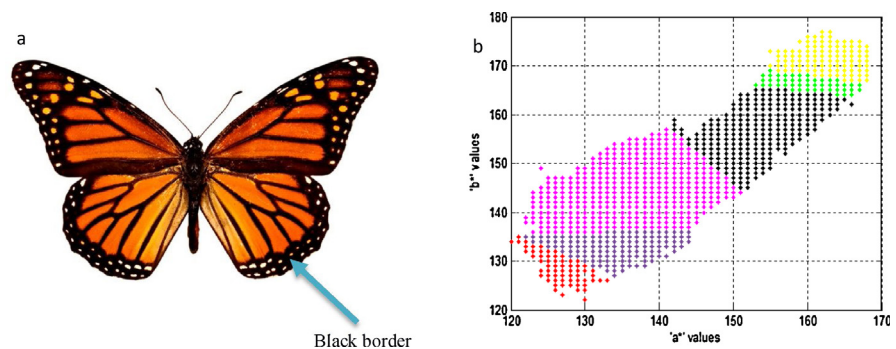


**Fig. 1.** (a) Bright view of the *Danaus plexippus*  $\times 20$  and (b) the CIELab color space of the wings of *Danaus plexippus*.

wings. For an automated classification, the k-means clustering algorithm with CIElab routine via the MATLAB image processing toolbox provides different colours as reported in Fig. 1(b).

Fig. 2(a–b) shows the SEM images of the *Danaus plexippus* wing at 100 and 2  $\mu\text{m}$ , respectively. Clearly, Fig. 2(b) shows the nanostructured ridges, separated by cross-ribs with different periodicities. The SEM image on a black border indicated with arrow shows the tip-end ridges displayed in Fig. 3(a).

### 3. Theory/calculation

To develop a theory of an electromagnetic wave propagation in a wing of a butterfly *Danaus plexippus*, part of SEM image was crop and presented in 3D (azimuth  $-25$ , elevation  $55$ ). Here, the waves travel along grooves (see Fig. 4) and are subject to a discrete translational symmetry.

The Eigen function modes of waves are given in the Bloch form [13] as

$$E_{k_z}(r) = E_n u_{k_z}(x) \quad (1)$$

with a periodic function  $u(z) = u(z + R)$ ,  $R = la$  ( $l$  is an integer,  $a$  is the lattice parameter),  $x$  is the direction of wave. Generation of corresponding eigenmode energy ( $E_n$ ) consider scattering around the groove.

The strategy for solving the scattering in and around the scales is to discretize the structure along the propagation direction. This is due to the homogeneity in the propagation direction ( $x$  – axis) where the wave is subjected to a translational symmetry with the ( $x$ ,  $y$ ) co-ordinates expressed in terms of the wavelength. The configuration is mapped onto a linear array with the index starting from 1 as the dielectric constant ( $\Delta\epsilon_i$ ) and the medium being ( $x_i, y_i$ ) as in Eq. (4);

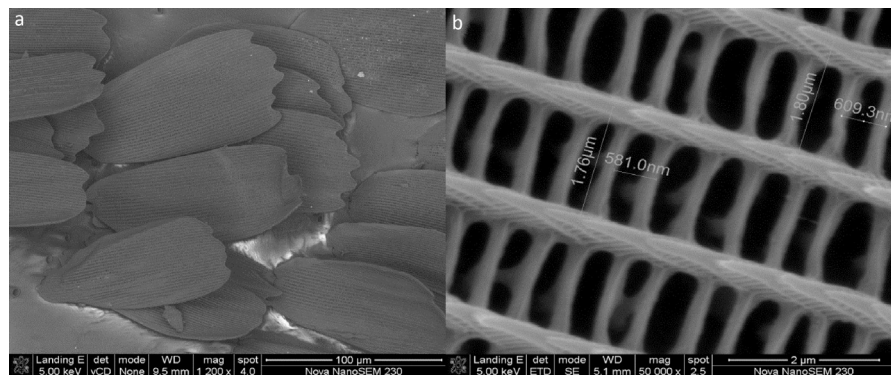


**Fig. 2.** (a) The SEM image of the wing showing cover and ground scales, (b) SEM image showing the longitudinal ridges and the cross-ribs.

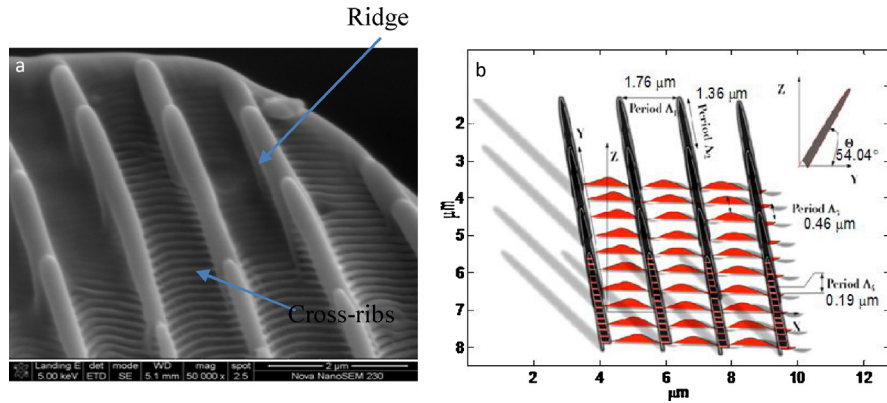


**Fig. 3.** (a) The tip end of scales showing longitudinal ridges and cross-ribs, (b) Detailed view of tip showing four periodic structures with different measurements showing mean length  $\Lambda_1 = \sim 1.76 \mu\text{m}$ ,  $\Lambda_2 = 1.36$ ,  $\Lambda_3 = 0.46 \mu\text{m}$ , and  $\Lambda_4 = 0.19 \mu\text{m}$ .

The scattering of electromagnetic fields in and outside the scales with a grid dielectric constant  $\Delta\epsilon(r) = \epsilon(r) - \epsilon_B$  is analyzed using the inhomogeneous Helmholtz equation [14] as

$$\nabla \times \nabla \times E(r) - k_0^2 \epsilon(r) E(r) = k_0^2 \Delta\epsilon(r) E(r) \tag{2}$$

where  $\Delta\epsilon(r) = 0$ , the background with the incident plane wave  $E^0(r) = E^0 e^{ikr}$  which is a solution of the homogeneous part of the Eq. (2). By assuming the scale to be a 2D scattering system, the tensor degrades to a scalar-tensor (GB). To be able to compute the scattered field in the time-harmonic case, the wave equation with a point source is (Refer Ref. [14])

$$\nabla \times \nabla \times E(r) - k_0^2 \epsilon_B G^B(r, r') = \delta(r - r') \tag{3}$$

with  $k_0^2 = k \cdot k$ ,

where  $k$  denotes the propagation vector. Solving Eq. (3) and combining with Eq. (2) gives (Refer Ref. [14])

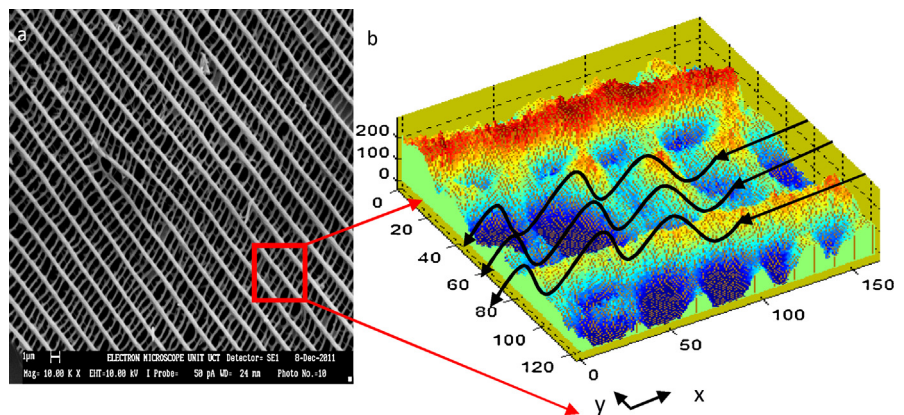


**Fig. 4.** (a) The SEM image of scales of Butterfly wings (b) showing crop section outputted in 3D.

$$\begin{matrix} \text{index} & \begin{bmatrix} 1 & 2 & 3 & 4 & 5 & 6 & 7 & 8 & \dots \end{bmatrix} \\ \Delta\varepsilon_i & \begin{bmatrix} 0 & 0 & 0 & 1.5 & 1.5 & 1.5 & 0 & 0 & \dots \end{bmatrix} \\ x_i & \begin{bmatrix} \lambda_2 & 2\lambda_2 & 3\lambda_2 & 4\lambda_2 & \lambda_2 & 2\lambda_2 & 3\lambda_2 & 4\lambda_2 & \dots \end{bmatrix} \\ y_i & \begin{bmatrix} \lambda_1 & \lambda_1 & \lambda_1 & \lambda_1 & 2\lambda_2 & 2\lambda_2 & 2\lambda_2 & 2\lambda_2 & \dots \end{bmatrix} \end{matrix} \tag{4}$$

$$E(r) = E^0(r) + \int G^B(r, r') k_0^2 \Delta\varepsilon(r') dr' \tag{5}$$

The above equation (Eq. (5)) enables the computation of the field in the background of scales where the solution inside the wing (scales) with  $\Delta\varepsilon(r) = 0$  is true outside. This is achieved by spitting the background and the scattered area with  $E_i = E(r_i)$  and  $G_{i,j}^B = G^B(r_i, r'_j)$ . Considering  $N$  to be the total number of cell elements of the area to be computed and  $V_j$  the cell volume area, Eq. (5) can be discretized as (Refer Ref. [14])

$$E_i = E_i^0 + \sum_{j=1, j \neq i}^N G_{i,j}^B k_0^2 \Delta\varepsilon_j E_j V_j + M_i k_0^2 \Delta\varepsilon_i E_i \tag{6}$$

$$G^B(r, r') = \frac{i}{4} H_0(k_\rho \rho) \exp(ik_z z) \tag{7}$$

Where  $H_\alpha(\rho)$  denotes Hankel functions [15] of the first kind:

$$M_i = \frac{i\pi\beta}{2} \gamma, \beta = 1 - \frac{k_z^2}{k_B^2}, \rho = \sqrt{(x - x^1)^2 + (y - y^1)^2} \text{ and [15]}$$

$$\gamma = \frac{R_i^{\text{eff}}}{k_\rho} H_1(k_\rho R_i^{\text{eff}}) + \frac{2i}{\pi k_\rho^2} \text{ with } k_\rho = \sqrt{k_x^2 + k_y^2}, R_i^{\text{eff}} = \left(\frac{V_i}{\pi}\right)^{1/2}, V_j = dx_i dy_i \text{ [15]}$$

The scattering of light by the wing is modeled from Eq. (6), by obtaining the geometry information using matrix analysis to simulate the wings surface and its relation to the scattered light. Numerical values used in the simulation include the wavelength of the trapped light, the dielectric constant, and the (x, y) – coordinates of the corresponding cells. By omitting  $V_j$ , in Eq. (6), a linear equation can be derived with  $N = 4$ , as (Refer Ref. [15])

$$\begin{pmatrix} E_1 \\ E_2 \\ E_3 \\ E_4 \end{pmatrix} = \begin{pmatrix} E_1^0 \\ E_2^0 \\ E_3^0 \\ E_4^0 \end{pmatrix} + k_0^2 \begin{pmatrix} M_1 \Delta\varepsilon_1 & G_{12}^B \Delta\varepsilon_2 & G_{13}^B \Delta\varepsilon_3 & G_{14}^B \Delta\varepsilon_4 \\ G_{21}^B \Delta\varepsilon_1 & M_2 \Delta\varepsilon_2 & G_{23}^B \Delta\varepsilon_3 & G_{24}^B \Delta\varepsilon_4 \\ G_{31}^B \Delta\varepsilon_1 & G_{32}^B \Delta\varepsilon_2 & M_3 \Delta\varepsilon_3 & G_{34}^B \Delta\varepsilon_4 \\ G_{41} \Delta\varepsilon_1 & G_{42}^B \Delta\varepsilon_2 & G_{43}^B \Delta\varepsilon_3 & M_4 \Delta\varepsilon_4 \end{pmatrix} \begin{pmatrix} E_1 \\ E_2 \\ E_3 \\ E_4 \end{pmatrix} \tag{8}$$

omitting  $k_0$  from Eq. (8) gives the matrix in the form  $A^* B = c$  and considering cell 1 and cell 3 as background give (Refer Ref. [15])

$$\begin{pmatrix} 1 & -G_{12}^B \Delta\varepsilon_2 & 0 & -G_{14}^B \Delta\varepsilon_4 \\ 0 & 1 - M_2 \Delta\varepsilon_2 & 0 & -G_{24}^B \Delta\varepsilon_4 \\ 0 & -G_{32}^B \Delta\varepsilon_2 & 1 & -G_{34}^B \Delta\varepsilon_4 \\ 0 & -G_{42}^B \Delta\varepsilon_2 & 0 & 1 - M_4 \Delta\varepsilon_4 \end{pmatrix} \begin{pmatrix} E_1 \\ E_2 \\ E_3 \\ E_4 \end{pmatrix} = \begin{pmatrix} E_1^0 \\ E_2^0 \\ E_3^0 \\ E_4^0 \end{pmatrix} \tag{9}$$

From Eq. (9), considering the cells 1 and 3 to be the background (see Fig. 4), leads to (Refer Ref. [15])

$$\begin{pmatrix} E_1 \\ E_3 \end{pmatrix} = \begin{pmatrix} E_1^0 \\ E_3^0 \end{pmatrix} + \begin{pmatrix} G_{12}^B \Delta \varepsilon_2 & G_{14}^B \Delta \varepsilon_4 \\ G_{32}^B \Delta \varepsilon_2 & G_{34}^B \Delta \varepsilon_4 \end{pmatrix} \begin{pmatrix} E_2 \\ E_4 \end{pmatrix} \tag{10}$$

whilst the cells 2 and 4 of the system are deduced from Eq. (9) as (Refer Ref. [15])

$$\begin{pmatrix} E_2^0 \\ E_4^0 \end{pmatrix} = \begin{pmatrix} E_2 \\ E_4 \end{pmatrix} \begin{pmatrix} 1 - M_2 \Delta \varepsilon_2 & -G_{24}^B \Delta \varepsilon_4 \\ -G_{42}^B \Delta \varepsilon_2 & 1 - M_4 \Delta \varepsilon_4 \end{pmatrix} \tag{11}$$

To evaluate Eq. (11) and calculate the scattering energies in the wing, we adopted the technique used in [12] and assumed the following;

- (i) The cells have the same shapes and sizes,
- (ii) The distance between each pair of cells is equal,
- (iii) The scattering configuration is mapped onto a linear geometry.

The geometric information needed is the x and y coordinates as well as the dielectric constant. This is obtained from Fig. 5 and mapped into Eq. (4). To obtain the geometry information, in order to compute the scattering and the corresponding energies, we varied the  $\lambda_1$  and  $\lambda_2$  in Eq. (4) to conform to the cross-ribs measurement as in Figs. 2 and 3. For n number of cells, a simple algorithm can be constructed to compute  $\rho$  in Eq. (7) such as

```
n = 1;
for i = number of cells
    rho(n,:) = sqrt(x(i,:)² + y(i,:)²)
n = n + 1
end
```

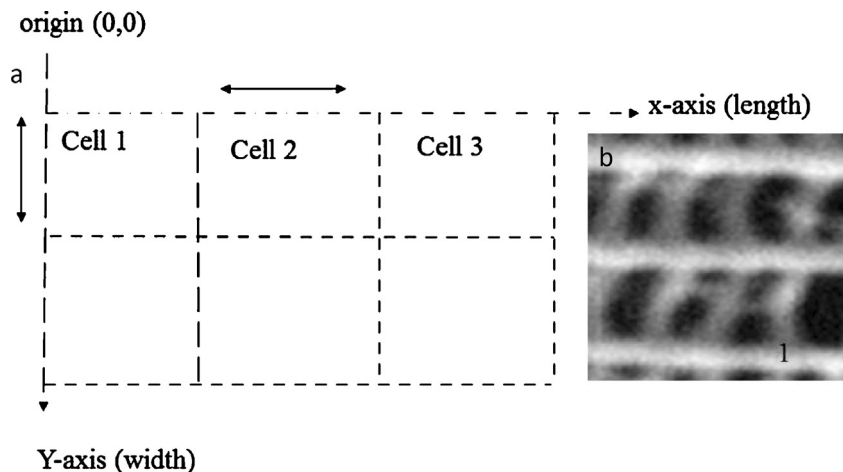


**Fig. 5.** (a) A 2D representation of scale image mapped onto (x, y) co-ordinates showing cells and wavelength along x and y, (b) SEM image of the scales oriented along the (x, y) co-ordinate.



The  $\rho$  values are used to compute the Green functions in Eq. (7). Deducing the diagonal elements  $M_i$  and the electromagnetic source term enables the computation of Eq. (11). The scattering of the electromagnetic waves through the cross-rib of the wings computed at different wavelengths are shown in Fig. 6 and the corresponding energy profile of the light is plotted in Fig. 7.

#### 4. Materials & methods

The wings of Butterflies *Danaus plexippus* were acquired from Cape Town city of Strand (South Africa) and carbon coated in an Emitech K950x high vacuum turbo

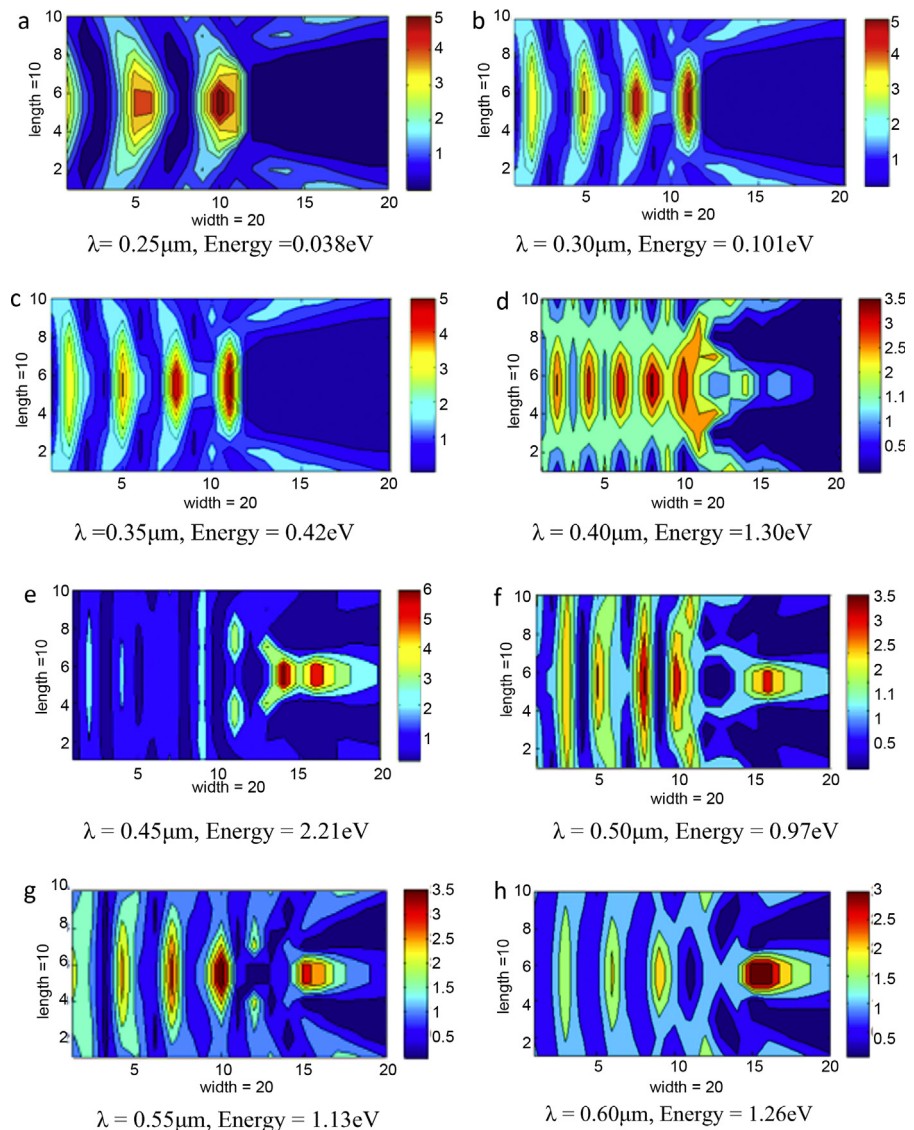


**Fig. 6.** (a–h) show the scattering patterns of translational movement of light in the groove over  $\Lambda$  and the calculated corresponding energies.

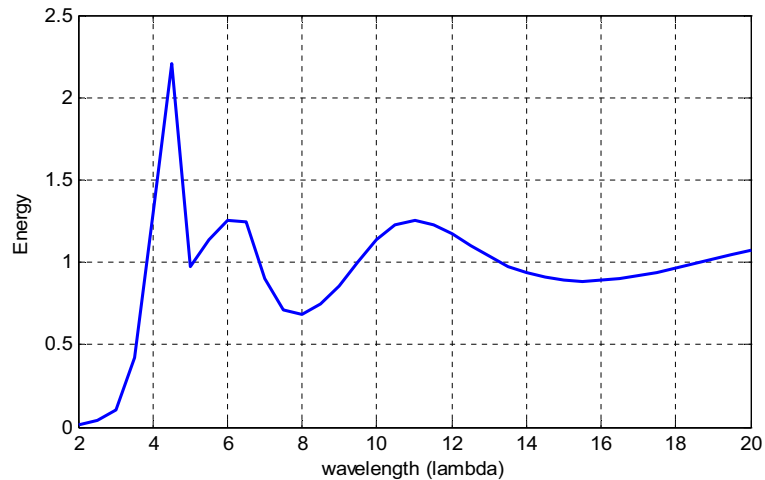


**Fig. 7.** The energy profile of the trapped light inside scales of wing indicating where resonance occurs at  $\lambda = 0.45 \mu\text{m}$  with energy = 2.21 eV.

system. The Nano-architectures of their scales were examined using the Nova NanoSEM Scanning Electron Microscope (SEM).

## 5. Conclusions

Using experimental measurements coupled with computer simulation, electromagnetic energies generated within the grooves (wing scales) of *Lepidoptera Danaus plexippus* wing are deduced. The Green tensor method used considers the scales as a 2D material and maps scattering configurations into (x, y) coordinates. Simulations of waves in grooves of scales were at specific wavelengths in accordance with measured cross-rib lengths. The maximum energy of 2.21 eV obtained at  $0.45 \mu\text{m}$  is similar to cross-rib spacing at the tip of wing. This gives insight into the design of bio-sensors of light and waveguide for photonic transmission.

## Declarations

### Author contribution statement

J. Sackey: Conceived and designed the experiments; Wrote the paper.

K. A. Dompheh: Analyzed and interpreted the data; Wrote the paper.

B. Mothudi: Contributed reagents, materials, analysis tools or data; Wrote the paper.

M. Maaza: Performed the experiments; Wrote the paper.

### Competing interest statement

The authors declare no conflict of interest.



## Funding statement

This work was supported by L'Oréal-UNESCO For Women in Science and Organization of Women in Science for the Developing World (OWSDW). As well as UNESCO-UNISA CHAIR IN NANOSCIENCE AND NANOTECHNOLOGY and NANOSCIENCES AFRICAN NETWORK (NANOAFNET).

## Additional information

No additional information is available for this paper.

## References

- [1] J. Boulenguez, S. Berthier, F. Leroy, Multiple scaled disorder in the photonic structure of *Morpho rhetenor* butterfly, *Appl. Phys. A* 106 (4) (2012) 1005–1011.
- [2] S. Berthier, Thermoregulation and spectral selectivity of the tropical butterfly *Prepona meander*: a remarkable example of temperature auto-regulation, *Appl. Phys. A* 80 (7) (2005) 1397–1400.
- [3] H. Ghiradella, Light and color on the wing: structural colors in butterflies and moths, *Appl. Opt.* 30 (24) (1991) 3492–3500.
- [4] G. Granet, B. Guizal, Efficient implementation of the coupled-wave method for metallic lamellar gratings in TM polarization, *J. Opt. Soc. Am. A* 13 (5) (1996) 1019–1023.
- [5] P. Lalanne, G.M. Morris, Highly improved convergence of the coupled-wave method for TM polarization, *J. Opt. Soc. Am. A* 13 (4) (1996) 779–784.
- [6] R.B. Srygley, R. Dudley, E.G. Oliveira, A.J. Riveros, Experimental evidence for a magnetic sense in neotropical migrating butterflies (Lepidoptera: Pieridae), *Anim. Behav.* 013 (2006) 183–191.
- [7] L. Brower, Monarch butterfly orientation: missing pieces of a magnificent puzzle, *J. Exp. Biol.* 93 (1996) 93–103.
- [8] S.M. Reppert, R.J. Gegear, C. Merlin, Navigational mechanisms of migrating monarch butterflies, *Trends Neurosci.* 33 (9) (2010) 399–406.
- [9] I. Sauman, A.D. Briscoe, H. Zhu, D. Shi, O. Froy, J. Stalleicken, S.M. Reppert, Connecting the navigational clock to sun compass input in monarch butterfly brain, *Neuron* 46 (3) (2005) 457–467.
- [10] C. Merlin, R.J. Gegear, S.M. Reppert, Antennal circadian clocks coordinate sun compass orientation in migratory monarch butterflies, *Science* 325 (5948) (2009) 1700–1704.

- [11] J.L. Yao-Bi, L. Nicolas, A. Nicolas, 2D electromagnetic scattering by simple shapes: a quantification of the error due to open boundary, *IEEE Trans. Magnet.* 29 (2) (1993) 1830–1834.
- [12] B. Hangartner, A 2D electromagnetic scattering solver for Matlab, 1 July 2002. [Online]. Available: <http://alphard.ethz.ch/hafner/Vorles/Numeric/2dscatterer.pdf>.
- [13] M. Saba, G.E. Schröder-Turk, Bloch modes and evanescent modes of photonic crystals: weak form solutions based on accurate interface triangulation, *Crystals* 5 (1) (2015) 14–44.
- [14] G. Arfken, *Mathematical Methods for Physicists*, Academic Press, Orlando, FL, 1985, pp. 529–530 eBook ISBN: 9781483277820.
- [15] U.D. Jentschura, E. Lötstedt, Numerical calculation of Bessel, Hankel and Airy functions, *Comput. Phys. Commun.* 183 (3) (2012) 506–519.